R. & M. No. 2944
(13,562, 14,606)
A.R.C. Technical Report

MINISTRY OF SUPPLY

AERONAUTICAL RESEARCH COUNCIL
REPORTS AND MEMORANDA

Technique for Flutter Tests using Ground-Launched Rockets, with Results for Unswept Wings

By

W. G. MOLYNEUX, B.Sc., F. RUDDLESDEN, A.M.I.E.I., and P. J. CUTT

LONDON: HER MAJESTY'S STATIONERY OFFICE
1956
PRICE 5*s* 6*d* NET

Technique for Flutter Tests using Ground-Launched Rockets, with Results for Unswept Wings

By

W. G. MOLYNEUX, B.Sc., F. RUDDLESDEN, A.M.I.E.I., and P. J. CUTT

COMMUNICATED BY THE PRINCIPAL DIRECTOR OF SCIENTIFIC RESEARCH (AIR), MINISTRY OF SUPPLY

Reports and Memoranda No. 2944*
November, 1951

Summary.—A technique for the investigation of wing flutter by means of ground-launched rockets is described. An important feature of the technique is that it can be used at high speeds, including the transonic range.

Model wings are attached to a solid-fuel rocket which has a miniature telemetry set housed in a detachable nose fairing. A vibration pick-up and break wires are fitted in the flutter model and these modulate the output of the telemetry set to transmit flutter information to a ground station. The rocket is fired over an open artillery range and its velocity-time curve is obtained by radio reflection Doppler equipment.

Results are given of tests on flutter models of unswept, untapered wings in the range of Mach number from 0·4 to 1·0.

The effects of longitudinal acceleration on the flutter are shown to be negligible for the range of acceleration and Mach number investigated, and the effect of compressibility is to reduce the margin of the measured speed above the speed calculated on the basis of incompressible flow theory from + 50 per cent at $M = 0{\cdot}4$ to — 25 per cent at $M = 0{\cdot}9$.

A wing torsional stiffness criterion which includes the Glauert function $\phi\,(M) = (1 - M^2)^{1/4}$ is shown to give a fair approximation to the test results.

1. *Introduction.*—Flight methods of flutter testing[1,2] provide a means of investigating flutter phenomena in the transonic range—a range which cannot easily be investigated in a wind tunnel. They also provide a useful alternative to tunnel tests for high-subsonic and supersonic conditions. This report describes a flight technique for flutter testing using rocket-propelled flutter models that are launched from the ground, and the technique is applied to flutter tests on unswept, untapered wings in the range of Mach number from 0·4 to 1·0.

The aims of the tests were to determine the effects of rocket acceleration and the effects of compressibility on wing flutter characteristics, and to determine a factor to be applied to the existing criterion for wing torsional stiffness[6,7] to allow for compressibility effects.

The investigation of acceleration effects shows them to be negligible in the range of acceleration from 19g to 31g, up to a Mach number of 0·65.

The effect of compressibility on flutter speed is determined from a comparison of the measured speed with the speed calculated using two-dimensional incompressible flow theory. This comparison shows that the margin of the measured speed above the theoretical speed is reduced from + 50 per cent at $M = 0{\cdot}4$ to — 25 per cent at $M = 0{\cdot}9$. The effect of compressibility on flutter frequency is to reduce it towards the wing bending frequency.

* R.A.E. Report Structures 72, received 6th December, 1950. R.A.E. Report Structures 118, received 2nd February, 1952.

A comparison of the measured flutter speeds with the speeds derived from the wing torsional stiffness criterion[7] shows that the Mach function $(1 - M^2)^{1/4}$ forms a reasonable boundary to the results up to $M = 0{\cdot}9$. A function to allow for wing density effects is also proposed. In its modified form the criterion is conservative with respect to the test results except in the region of $M = 0{\cdot}8$, where it is slightly unconservative.

Further investigations are to be made on wings of different plan-forms, and the technique is to be developed for *ad-hoc* tests on scale models of specific aircraft.

2. *Details of the Rocket Model.*—A complete rocket model is shown in Figs. 1 and 2. The model was assembled so that the centre of gravity of the complete rocket was at the wing leading edge, to ensure an adequate margin of pitching stability in flight. The average launching weight of a complete model with 3-in. rocket was 55 lb, and at this weight the acceleration of the model during the 1·6 sec burning time was about 24*g* giving a peak velocity of about 1,200 ft/sec. The ratios of (complete model weight): (wing weight) and (complete pitching inertia): (wing pitching inertia) were not less than 5 : 1 and 120 : 1 respectively for any of the models, and were considered adequate to ensure that the flutter obtained approximated to the flutter of a wing fixed at the root. To extend the Mach number range, two of the models were tested using a 5-in. rocket in place of the 3-in. rocket normally used. The launching weight of these models was 140 lb; the acceleration during the burning period of 1·6 sec was about 40*g* and the peak velocity was about 2,000 ft/sec.

2.1. *Telemetry Equipment.*—The telemetry equipment was developed by Guided Weapons Department, Royal Aircraft Establishment. The part carried on the rocket (Fig. 3) was a single channel 465 Mc/sec transmitter with its output amplitude modulated at a frequency of 150 ± 15 Kc/sec. The variation of ± 15 Kc/sec corresponded to the range of variation of the inductance of the vibration pick-up, and this variation was recorded as a continuous trace at a ground station. The weight of the unit was 2·5 lb.

2.2. *Doppler Equipment.*—The velocity of the model was obtained by using a radio reflection Doppler system in which a signal at 212 Mc/sec was transmitted to the model and was reflected back to the transmitting station. The difference in frequency of the transmitted and received signals was a measure of the speed at which the model receded from the transmitter, and this difference was recorded. A frequency difference ranging from 0 to 1000 c/sec corresponded to a velocity of recession ranging from 0 to 2,320 ft/sec. The velocity normally required some correction to allow for trajectory and line of fire of the test vehicle relative to the transmitter, and could be obtained to better than 0·5 per cent accuracy.

2.3. *Vibration Pick-up.*—A variable inductance accelerometer-type pick-up was used (Fig. 4). It had a natural frequency of about 100 c/sec and was designed for a range of acceleration of ± 20*g*. Oil damping was provided to damp the natural frequency oscillations and irregular vibrations experienced in flight.

2.4. *Wing Details.*—The external dimensions of all the wings tested were as follows:

Length (root to tip) ..	= 2·0 ft
Chord	= 1·0 ft
Aspect ratio	= 4·4 (4·6 for 5-in. rocket models)
Thickness/chord ..	= 0·10
Wing section — RAE 101	

Three types of wing structure were used in the course of the tests (*see* Fig. 5). Wings of stressed-skin construction (models No. 1101 to 1115) were used for the initial development of the rocket model technique and to investigate the effects of acceleration on flutter characteristics. The construction consisted of a light wooden framework to which the skin was glued. A variation of wing stiffness could be obtained by using skins of plywood, metal and plastic. The construction

was found to be generally unsuitable for rocket work since the wing flexural-axis location could not be controlled, models were easily damaged and there were glueing difficulties which resulted in skin failures in flight due to aerodynamic suction.

To overcome these difficulties a solid wing construction was developed. This consisted of a plywood sheet cut to the wing plan-form, carrying a metal spar at 30 per cent of the chord aft of the leading edge, four equally spaced ash ribs and the wing contour filled in with balsa wood. Lead strips glued to the plywood determined the wing inertia-axis position, the location of the spar determined the flexural-axis position and by varying the gauge of the spar material a variation of wing stiffness could be obtained. This construction was used for models 1116 to 1128. Flight tests demonstrated that the flexural axis position was too far aft so that, for models designed to flutter at high speeds, divergence occurred before flutter. There was also a tendency for the nose structure to break away from the spar.

The construction was modified to bring the spar location to 25 per cent chord aft of the leading edge and a plywood skin nose was added forward of the 45 per cent chord line. The divergence characteristics were improved and the nose weakness eliminated. In addition a reduction of wing stiffness could be made after construction by cutting chordwise slots in the stressed-skin nose. Models 1136 to 1143 were of this construction and were used for the high Mach number tests.

3. *Test Procedure.*—Static measurements of the wing elastic and inertia characteristics were made on all the models. Resonance tests were also made on many of the models to determine the wing natural frequencies.

All models were launched at an elevation of $12\frac{1}{2}$ deg. A continuous photographic record was obtained of the transmitted signals from the vibration pick-up in one wing of each model, and the flight path of the model was followed by radio reflection Doppler equipment and by ciné-cameras.

Wing components were subsequently recovered from the range so that the failures could be examined. Pick-ups recovered with the wings were used in further tests.

3.1. *Test Results.*—Photographic records were obtained from the telemetry and Doppler stations and from the range ciné-cameras. In general, correlation of the telemetry and Doppler results gave the required flutter information, whilst the ciné-camera record provided a useful check. Results for a typical model are shown in Figs. 6, 7 and 8. Fig. 6 gives three consecutive frames of the rear view camera record and shows the flutter failure. The wing is seen to disintegrate into small fragments. Fig. 7 shows the telemetry record of the wing oscillations in flight. Flutter is presumed to commence when the oscillations are of regular frequency and divergent amplitude. The rapid divergence of the flutter oscillations is shown by the fact that the limit of travel of the pick-up (indicated by the flat-topped curves) is reached after about three cycles and the wing fails after five cycles. However, at this point the speed is considerably greater than at commencement of flutter. Fig. 8 is the velocity-time curve derived from Doppler measurements. Irregularities in the region of flutter failure are probably due to Doppler errors resulting from dispersed reflection from the disintegrated model. From Figs. 7 and 8 the results obtained are:

Flutter frequency	= 58 c/sec
Speed of model at beginning of flutter ..	= 650 ft/sec
Speed of model at wing failure	= 760 ft/sec
Acceleration of model during flutter ..	= 26g.

4. *Theoretical Investigation.*—Theoretical estimates of flutter speed and frequency at ground level were obtained for each model for comparison with the test results. The modes chosen were

the decoupled flexural and torsional fundamental modes of a fixed-root uniform wing, and they were used in conjunction with the static measurements of the wing elastic and inertia characteristics. Calculations were made using two-dimensional vortex-sheet theory derivatives for both incompressible and compressible flow; the former for comparison with the test results to obtain the effect of compressibility, the latter for correlation between compressible flow theory and experiment. No corrections were made for aspect-ratio effects. The derivative values used were obtained from Refs. 3 and 4. Ref. 3 gives derivative values for the range of Mach number from 0 to 0·8 only, but for some of the models values were required within the range of Mach number from 0·8 to 1·0, and these were obtained from Ref. 4. It is probable that the derivative values are considerably in error for Mach numbers approaching unity since in their determination no account has been taken of shock-wave formation. However, the results of calculations made using these derivatives provide an explanation for unique features of the records from models which fluttered at high Mach number (*see* section 5.3).

The flutter equations were solved by the use of an electronic simulator[5]. In general the values of frequency parameter and Mach number assumed for the derivatives were balanced with the values derived from the solution. For the calculations using compressible-flow derivatives the method used to balance the Mach number may be explained by reference to Fig. 11, which shows the results for four of the higher Mach number model wings (1136 to 1139 inclusive). The first diagram of Fig. 11 shows a curve for each model giving the variation of calculated flutter speed with the Mach number assumed in the evaluation of the derivatives. On the same diagram is drawn the straight line giving the relationship between speed and Mach number for actual flight conditions. Intersections of this straight line with the calculated flutter curve then give the theoretical critical flutter conditions in which the Mach number appropriate to the flutter speed is the same as that assumed in the evaluation of the derivatives. In some cases, as for instance the three upper curves of Fig. 11, balance of Mach number could not be achieved because no such intersection occurred. It was then assumed that the theoretical flutter speed was given by the minimum of the flutter curve.

5. *Discussion of Results.*—5.1. *General.*—The experimental and theoretical results are given in Table 1. A total of thirty-two models were tested and of these thirty-one were designed for flutter tests and one (model 1126) for divergence tests. Records of flutter oscillations were obtained from twenty-two of the flutter models, and five others probably fluttered though records were not obtained due to telemetry failure; the remaining four failed under aerodynamic suction loads. The elastic and inertia characteristics of the models were varied over a wide range, but an increase in flutter speed was obtained primarily by an increase of wing stiffness. The records of flight characteristics from the wing vibration pick-ups were of five distinct types as follows (*see* Fig. 9):

1. Wing divergence failure.
2. Flutter oscillations followed by wing-divergence failure.
3. Flutter oscillations leading to wing-flutter failure during the rocket acceleration period.
4. Flutter oscillations during the rocket acceleration period dying out as the speed increases, and subsequently reappearing during the deceleration period and leading to wing-flutter failure.
5. Flutter oscillations during the acceleration and deceleration periods without wing failure.

In general, the wings were designed to ensure that flutter occurred before divergence, and a record of type 1 was obtained only on model 1126 which was designed to demonstrate divergence failure. Records of type 2 were fairly common, particularly for the models tested at high Mach number, and this despite the fact that for the latter models the wing flexural axis was at about 25 per cent of the wing chord aft of the leading edge. Type 3 records were those most generally

obtained. Records of types 4 and 5 were obtained only on models which fluttered in the range of Mach number from 0·8 to 1·0 and their significance is discussed in section 5.3.

5.2. *The Effects of Longitudinal Acceleration.*—For this investigation two sets of identical models were constructed and these were tested on rockets ballasted to different launching weights to cover a range of acceleration from 19*g* to 31*g*. This range of acceleration was fixed by limitations in range facilities and the total impulse of the rocket. The first set of models (Nos. 1102, 1112, 1113, 1114, 1115) fluttered at a Mach number of about 0·58 and the second set (Nos. 1108, 1109, 1110, 1111) fluttered at a Mach number of about 0·65.

Although the models were designed to be identical, differences in structural characteristics were obtained (*see* Table 1). These differences were levelled out by expressing the experimental results as a ratio to the compressible flow theoretical results, and this ratio is plotted against rocket acceleration in Fig. 10. It can be seen that for the range of acceleration investigated there is no noticeable effect of acceleration on either flutter speed or frequency.

5.3. *The Effects of Compressibility.*—The records from the wing vibration pick-ups showed that as the Mach number at flutter increased, the flutter frequency was reduced towards the wing fundamental bending frequency, and for the range of Mach number from 0·8 to 1·0 it was in some cases slightly less than the bending frequency. The high Mach number records also indicated that there was a finite speed range for flutter, with no flutter at speeds beyond the upper limit of this range, up to the peak speed of the model.

The results of the theoretical investigation made on models 1136 to 1139 for the range of Mach number from 0 to 1·0 are plotted in Fig. 11. The flutter speed *vs.* Mach number curves are the flutter boundaries (*see* section 4) for the various models, and the line through the origin and the point $V=1117$ ft/sec, $M=1\cdot0$ represents the rocket flight conditions on a standard day. This line intersects the flutter boundary of model 1139 at the points $V=875$ ft/sec and $V=1000$ ft/sec indicating that within this speed range the model will flutter and at higher and lower speeds there will be no flutter. Obviously the acceleration of the model could be such that the flutter region was traversed before the flutter developed to wing failure. The flutter oscillations would then die away to re-appear as the model decelerated through the flutter region and the occurrence of wing failure during deceleration would depend on the rate of deceleration through the flutter region. A pick-up record with the above characteristics is typical of those obtained for the high Mach number tests (records 4 and 5, Fig. 9). There is no intersection of the rocket flight line with the flutter boundaries of models 1136, 1137 and 1138, but in practice model 1136 fluttered during the acceleration and deceleration periods without wing failure, model 1137 fluttered during the acceleration and deceleration periods with wing failure during deceleration, and models 1138 and 1139 fluttered to destruction during the acceleration period. Generally speaking, therefore, the severity of the flutter encountered in the test is reflected in the nearness of the theoretical curve to the rocket line.

The theoretical effect of compressibility on flutter frequency is to reduce this frequency towards the wing bending frequency with increasing Mach number. The trend is less pronounced than is obtained experimentally (*see* Table 1). However, close agreement of theory with experiment is not to be expected, particularly in view of the uncertainties attached to the derivative values at high Mach number.

The experimental results are expressed as ratios of the theoretical results in Table 1, and these ratios are plotted against Mach number at flutter in Fig. 12. The comparison of experiment with incompressible-flow theory shows that the margin of the experimental speed above the theoretical speed is reduced from about + 50 per cent at $M=0\cdot4$ to − 25 per cent, at $M=0\cdot9$; a similar comparison with compressible flow theory gives margins of about + 50 per cent at $M=0\cdot4$ reducing to − 12 per cent at $M=0\cdot9$. In both cases the frequency ratio shows a marked reduction with increasing Mach number.

5.4. *Wing Torsional Stiffness Criterion.*—A criterion for wing torsional stiffness has been proposed[6,7] of the form:—

$$\frac{1}{V}\left(\frac{m_0}{\rho_0 dc_m^2}\right)^{1/2} = 0{\cdot}9\,\frac{(g-0{\cdot}1)(1{\cdot}3-h)}{(0{\cdot}9-0{\cdot}33k)(1-0{\cdot}1r)\sec^{3/2}(\beta-\frac{1}{16}\pi)}. \qquad (1)$$

(*See* List of symbols.)

The experimental data of the present report form a basis for the extension of the above criterion to include the effects of compressibility.

The flutter speeds determined on the basis of the criterion are given in Table 2, and the ratio of experimental flutter speed to criterion flutter speed is plotted against Mach number at flutter in Fig. 13. The curve of the Glauert function $\phi(M) = (1-M^2)^{1/4}$ is also shown, and it can be seen that this curve forms a reasonable boundary to the results, with the following limitations:

$$\begin{aligned}\phi(M) &= (1-M^2)^{1/4},\ 0 < M < 0{\cdot}9\\ &= 0{\cdot}66, \qquad 0{\cdot}9 < M < 1{\cdot}0\,.\end{aligned}$$

The discrepancy between this boundary and the experimental results is greatest for the results at the lower Mach numbers. However, these results are mainly for wings of low relative density ($\sigma_w < 10$), and there is no allowance for variation of wing density in the criterion. An investigation of the effect of wing relative density on flutter speed has been made for one of these wings[5], and from these results a relative density factor to be applied to the criterion has been derived. This factor is of the form:

$$\phi(\sigma_w) = \left(0{\cdot}95 + \frac{1{\cdot}3}{\sigma_w}\right).$$

By including this factor the agreement of the results with the boundary formed by $\phi(M) = (1-M^2)^{1/4}$ is improved.

5.4.1. *Suggested modified criterion.*—On the basis of the above results a modified criterion is suggested of the form:

$$\frac{1}{V}\left(\frac{m_0}{\rho_0 dc_m^2}\right)^{1/2} = \frac{0{\cdot}9(g-0{\cdot}1)(1{\cdot}3-h)}{(0{\cdot}9-0{\cdot}33k)(1-0{\cdot}1r)\left(0{\cdot}95+\frac{1{\cdot}3}{\sigma_w}\right)\phi(M)\sec^{3/2}\left(\beta-\frac{\pi}{16}\right)}$$

$$\begin{aligned}\phi(M) &= (1-M^2)^{1/4},\ 0 < M < 0{\cdot}9\\ &= 0{\cdot}66\,, \qquad 0{\cdot}9 < M < 1{\cdot}0\,.\end{aligned}$$

It should be noted that the suggested modifications are based on results for unswept wings of one particular plan-form. Further experimental and theoretical verification is required for their acceptance.

6. *Conclusions.*—The technique of using ground-launched rockets provides a means for flutter investigation at high-subsonic and supersonic speeds, including transonic conditions. The technique can be applied to the empirical determination of the effects of relevant parameters on the flutter characteristics and to the development of more accurate theoretical prediction of flutter characteristics.

The general conclusions from tests on unswept, untapered wings are as follows:

(*a*) The effects of acceleration on flutter characteristics are negligible for these models, within the range of acceleration from 19*g* to 31*g*.

(b) The effect of compressibility on the fixed-root flutter speed is to reduce the margin of the true flutter speed above the speed calculated using two-dimensional incompressible flow theory from about + 50 per cent at $M = 0{\cdot}4$ to − 25 per cent at $M = 0{\cdot}9$.

(*c*) The effect of compressibility on the flutter frequency is to reduce this frequency towards the wing fundamental bending frequency.

(*d*) Modifications to the wing torsional stiffness criterion are suggested to allow for the effects of compressibility and wing relative density on flutter speed. The suggested compressibility function is:

$$\begin{aligned}\phi(M) &= (1 - M^2)^{1/4}, \; 0 < M < 0{\cdot}9 \\ &= 0{\cdot}66\,, \qquad 0{\cdot}9 < M < 1{\cdot}0\,.\end{aligned}$$

The suggested wing relative density function is:

$$\phi(\sigma_w) = \left(0{\cdot}95 + \frac{1{\cdot}3}{\sigma_w}\right)$$

7. *Further Developments.*—Similar investigations to the above are to be made on wings of different plan-forms. Tests are in progress on untapered wings swept back to an angle of 40 deg. The technique is also being developed for *ad hoc* flutter tests on scale models of specific aircraft.

Acknowledgment.—Acknowledgments are due to the staff of Guided Weapons Department, Trials Division, for assistance given in the calibration and testing of these models.

TABLE 1

Experimental and Theoretical Results

Model No.	Experimental results														Theoretical results						Ratio: Experiment / Theory			
															Incompressible			Compressible						
	l_ϕ	m_θ	h	g	K_G	w	n_B	n_T	V_C	n_C	ω_C	M_C	f_C/G	V_F	V_1	n_1	ω_1	V_2	n_2	ω_2	V_C/V_1	n_C/n_1	V_C/V_2	n_C/n_2
1101	1290	680	0·25	0·47	0·30	1·02	22	88	740	43	0·36	0·66	26	835	537	47	0·55	540	40	0·47	1·38	0·91	1·37	1·08
1102	1420	533	0·29	0·47	0·29	0·55	30	96	650	58	0·56	0·58	26	760	496	59	0·74	508	53	0·66	1·31	0·98	1·28	1·09
1103	3580	2180	0	0·47	0·29	0·68	39	159						940										
1104	3180	1890	0	0·47	0·29	0·61	38	148						960										
1105	3050	1940	0	0·47	0·29	0·66	35	134						965										
1106	3050	1880	0	0·47	0·29	0·59	35	126						950										
1108	1930	707	0·34	0·47	0·29	0·71			740	60	0·51	0·66	28	755	549	61	0·69	578	55	0·59	1·35	0·98	1·28	1·09
1109	1830	732	0·26	0·47	0·29	0·71								840	534	61	0·72	566	54	0·60				
1110	1900	702	0·24	0·47	0·29	0·71			720	60	0·52	0·64	25	780	520	59	0·72	547	54	0·62	1·38	1·02	1·31	1·10
1111	1650	712	0·24	0·47	0·29	0·71			715	59	0·52	0·64	22	790	528	60	0·71	558	54	0·61	1·35	0·98	1·28	1·09
1112	1560	546	0·22	0·47	0·29	0·55	32	96	640	60	0·58	0·57	19	710	474	57	0·75	495	53	0·67	1·35	1·05	1·29	1·13
1113	1690	532	0·20	0·47	0·29	0·55	33	96	655	58	0·56	0·59	23	760	462	61	0·83	470	54	0·73	1·42	0·95	1·39	1·07
1114	1630	583	0·23	0·47	0·29	0·55	33	98	640	58	0·57	0·57	23	760	509	60	0·74	516	56	0·68	1·26	0·97	1·24	1·04
1115	1500	568	0·26	0·47	0·29	0·55	31	97	640	60	0·59	0·57	31	765	505	61	0·76	510	55	0·67	1·27	0·98	1·25	1·09
1116	1650	351	0·30	0·33	0·29	1·12								740	581	34	0·36	592	32	0·34				
1117	1450	315	0·32	0·47	0·28	1·00	23	61	495	34	0·31	0·44	23	565	346	37	0·68	340	32	0·59	1·43	0·92	1·46	1·06
1118	1600	394	0·31	0·39	0·31	1·40			590	25	0·26	0·53	27	730	452	31	0·43	440	29	0·42	1·31	0·81	1·34	0·86
1119	2180	382	0·30	0·47	0·28	1·16								649	371	39	0·65	360	34	0·58				
1121	2110	395	0·29	0·34	0·29	1·25			655	32	0·33	0·59	25	800	560	35	0·39	546	33	0·38	1·17	0·91	1·20	0·97
1122	2500	384	0·30	0·47	0·28	1·40			520	35	0·40	0·47	25	650	362	35	0·60	354	32	0·57	1·44	1·00	1·47	1·09
1123	1850	417	0·29	0·40	0·31	1·24			610	32	0·33	0·55	22	740	473	36	0·48	463	33	0·45	1·29	0·89	1·32	0·97
1126	3860	4050	0·36	0·47	0·28	2·15								1130										
1127	4370	906	0·32	0·38	0·22	1·78	31	95	845	38	0·28	0·79	25	1010	832	47	0·35	811	41	0·32	1·02	0·81	1·04	0·93
1128	3130	1180	0·30	0·40	0·29	2·29	25	94						1005	821	39	0·30	810	36	0·28				
1136	5090	2290	0·26	0·37	0·25	1·96	27	130	1090	27	0·16	0·98	9		1340	65	0·30	1180	51	0·27	0·81	0·42	0·92	0·53
1137	4700	1950	0·25	0·38	0·25	1·89	31	120	1010	28	0·17	0·90	14	1000	1160	59	0·32	1000	47	0·29	0·87	0·47	1·01	0·60
1138	4000	1940	0·26	0·38	0·25	1·78	33	119	945	32	0·21	0·85	23	1020	1216	61	0·31	1060	49	0·29	0·78	0·52	0·89	0·65
1139	3350	1530	0·25	0·39	0·27	1·67	31	112	856	34	0·25	0·77	25	985	993	55	0·35	875	43	0·31	0·86	0·62	0·98	0·79
1140	2210	1270	0·24	0·36	0·24	2·31	24	99	875	24	0·17	0·78	26	1040	912	43	0·29	766	34	0·28	0·96	0·56	1·14	0·71
1141	5590	1420	0·22	0·38	0·25	2·00	27	107						900	832	54	0·41	700	45	0·40				
1142	4850	1550	0·23	0·37	0·25	2·13	28	104	945	40	0·27	0·85	43	1050	891	51	0·36	773	41	0·33	1·06	0·78	1·22	0·97
1143	3590	1450	0·22	0·38	0·26	1·83	27	114	835	28	0·20	0·75	42	990	850	54	0·40	731	41	0·35	0·98	0·52	1·14	0·68

Notation

l_ϕ Wing bending stiffness measured at 0·7s, lb ft/radn
m_θ Wing twisting stiffness measured at 0·7s, lb ft/radn
h Distance of wing flexural axis aft of leading edge ÷ wing chord
g Distance of wing inertia axis aft of leading edge ÷ wing chord
K_G Radius of gyration of wing section about inertia axis ÷ wing chord
w Wing weight per foot run, lb/ft
n_B Wing fundamental flexure frequency, cycles/sec
n_T Wing fundamental torsion frequency, cycles/sec
G Gravitational acceleration, ft/sec²

V_C Critical flutter speed, ft/sec
n_C Flutter frequency, cycles/sec
ω_C Flutter frequency parameter
M_C Mach number at critical flutter speed
f_C Rocket acceleration at critical flutter speed, ft/sec²
V_F Speed at wing failure, ft/sec
$V_{1,2}$ Calculated flutter speeds, ft/sec
$n_{1,2}$ Calculated flutter frequencies, cycles/sec
$\omega_{1,2}$ Calculated flutter frequency parameters

TABLE 2

Comparison of Experimental and Criterion Flutter Speeds

Model No.	l_ϕ	m_θ	r	g	h	$\rho_w G$ (lb/cu ft)	V_A	V_B	V_C	M_C	$\frac{V_C}{V_A}$	$\frac{V_C}{V_B}$
1101	1290	680	0·59	0·47	0·25	1·02	631	662	740	0·66	1·17	1·12
1102	1420	533	0·84	0·47	0·29	0·55	563	638	650	0·58	1·15	1·02
1103	3580	2180	0·51	0·47	0	0·68	920	1010				
1104	3180	1890	0·52	0·47	0	0·61	855	953				
1105	3040	1940	0·49	0·47	0	0·66	869	960				
1106	3050	1880	0·50	0·47	0	0·59	856	958				
1108	1930	707	0·85	0·47	0·34	0·71	684	747	740	0·66	1·08	0·99
1109	1830	732	0·77	0·47	0·26	0·71	648	707				
1110	1900	702	0·84	0·47	0·24	0·71	618	675	720	0·64	1·16	1·07
1111	1660	712	0·72	0·47	0·24	0·71	628	686	715	0·64	1·14	1·04
1112	1560	546	0·88	0·47	0·22	0·55	534	605	640	0·57	1·20	1·06
1113	1690	532	0·98	0·47	0·20	0·55	511	578	655	0·59	1·28	1·13
1114	1630	583	0·86	0·47	0·23	0·55	556	630	640	0·57	1·15	1·02
1115	1500	568	0·81	0·47	0·26	0·55	567	642	640	0·57	1·13	1·00
1116	1650	351	1·45	0·33	0·30	1·12	694	721				
1117	1450	315	1·42	0·47	0·32	1·00	418	440	495	0·44	1·18	1·12
1118	1600	394	1·26	0·39	0·31	1·40	603	617	590	0·53	0·98	0·96
1119	2180	382	1·76	0·47	0·30	1·16	434	450				
1121	2110	395	1·65	0·34	0·29	1·25	684	705	655	0·59	0·96	0·93
1122	2500	384	2·01	0·47	0·30	1·40	423	433	520	0·47	1·23	1·20
1123	1850	417	1·37	0·40	0·29	1·24	581	599	610	0·55	1·05	1·02
1126	3860	4050	0·29	0·47	0·36	2·15	1780	1770				
1127	4370	906	1·48	0·38	0·32	1·78	932	937	845	0·79	0·91	0·90
1128	3130	1180	0·82	0·40	0·30	2·29	1050	1040				
1136	5090	2290	0·69	0·37	0·26	1·96	1590	1590	1090	0·98	0·69	0·69
1137	4700	1950	0·75	0·38	0·25	1·86	1380	1383	1010	0·90	0·73	0·73
1138	4000	1940	0·64	0·38	0·26	1·78	1410	1417	945	0·85	0·67	0·67
1139	3350	1530	0·67	0·39	0·25	1·67	1200	1212	856	0·77	0·70	0·71
1140	2210	1270	0·54	0·36	0·24	2·31	1220	1210	875	0·78	0·72	0·72
1141	5590	1420	1·22	0·38	0·22	2·00	1110	1110				
1142	4850	1550	0·97	0·37	0·23	2·13	1230	1230	945	0·85	0·77	0·77
1143	3590	1450	0·77	0·38	0·22	1·83	1160	1166	835	0·75	0·72	0·72

LIST OF SYMBOLS

$$V_A = \left(\frac{m_0}{\rho_0 d c_m^2}\right)^{1/2} \frac{(0{\cdot}9 - 0{\cdot}33k)(1 - 0{\cdot}1r)\ \sec^{3/2}\left(\beta - \frac{\pi}{16}\right)}{0{\cdot}9(g - 0{\cdot}1)(1{\cdot}3 - h)}$$

$$V_B \quad \left(\frac{m_0}{\rho_0 d c_m^2}\right)^{1/2} \frac{(0{\cdot}9 - 0{\cdot}33k)(1 - 0{\cdot}1r)\left(0{\cdot}95 + \frac{1{\cdot}3}{\sigma_w}\right)\sec^{3/2}\left(\beta - \frac{\pi}{16}\right)}{0{\cdot}9(g - 0{\cdot}1)(1{\cdot}3 - h)}$$

V_C Critical flutter speed, ft/sec

M_C Mach number at critical flutter speed

g Gravitational acceleration, ft/sec^2

c_m Wing mean chord, ft

d Wing length to equivalent tip ($= 0{\cdot}9s$)

g Distance of inertia axis aft of leading edge ÷ wing chord

k Wing taper ratio $\left(= \frac{\text{Tip chord}}{\text{Root chord}}\right)$

h Distance of flexural axis aft of leading edge ÷ wing chord

l_ϕ Wing flexural stiffness measured at $0{\cdot}7s$, lb ft/radn

m_0 Wing torsional stiffness measurement at $0{\cdot}7s$, lb ft/radn

r Stiffness ratio $\left(= \frac{l_\phi}{d^3} \Big/ \frac{m_0}{dc_m^2}\right)$

s Wing length from root to tip, ft

β Angle of sweepback, radians

ρ_0 Air density at sea-level, slugs/cu ft

ρ_w Wing density in slugs/cu ft $\left(= \frac{\text{Mass of one wing}}{sc_m^2}\right)$

σ_w Wing relative density $\left(= \frac{\text{Density of wing}}{\text{Density of surrounding air}}\right)$

REFERENCES

No.	*Author*	*Title, etc.*
1	F. Smith	Note on use of flight models for investigation of flutter. R.A.E. Tech. Note Structures 11. A.R.C. 11,404. March, 1948. (Unpublished.)
2	W. G. Molyneux and E. G. Chapple.	Flutter experiments with freely falling models at high subsonic speeds. R.A.E. Report Structures 67. A.R.C. 13,722. May, 1950.
3	I. T. Minhinnick	Subsonic aerodynamic flutter derivatives for wings and control surfaces. R.A.E. Report Structures 87. A.R.C. 14,228. July, 1950.
4	P. F. Jordan	Aerodynamic flutter coefficients for subsonic, sonic and supersonic flow (linear two-dimensional theory). R. & M. 2932. April, 1953.
5	F. Smith and W. D. T. Hicks ..	The design of a simple electronic flutter simulator. R.A.E. Report Structures 74. A.R.C. 13,563. July, 1950.
6	A. R. Collar, E. G. Broadbent and E. B. Puttick	An elaboration of the criterion for wing torsional stiffness. R. & M. 2154. January, 1946.
7	W. G. Molyneux	The flutter of swept and unswept wings with fixed root conditions. R. & M. 2796. January, 1950.

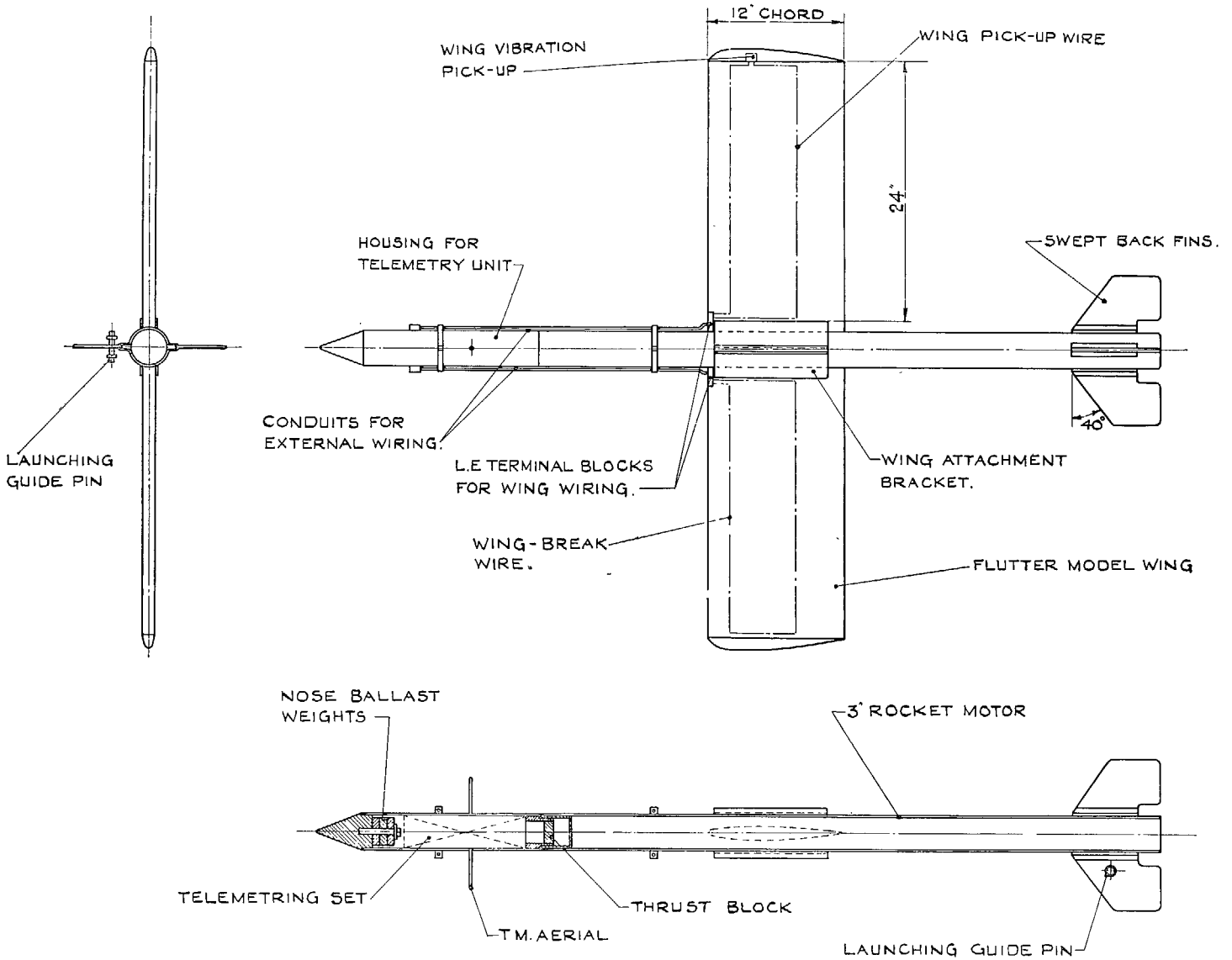

FIG. 1. General arrangement of rocket model. Third angle projection.

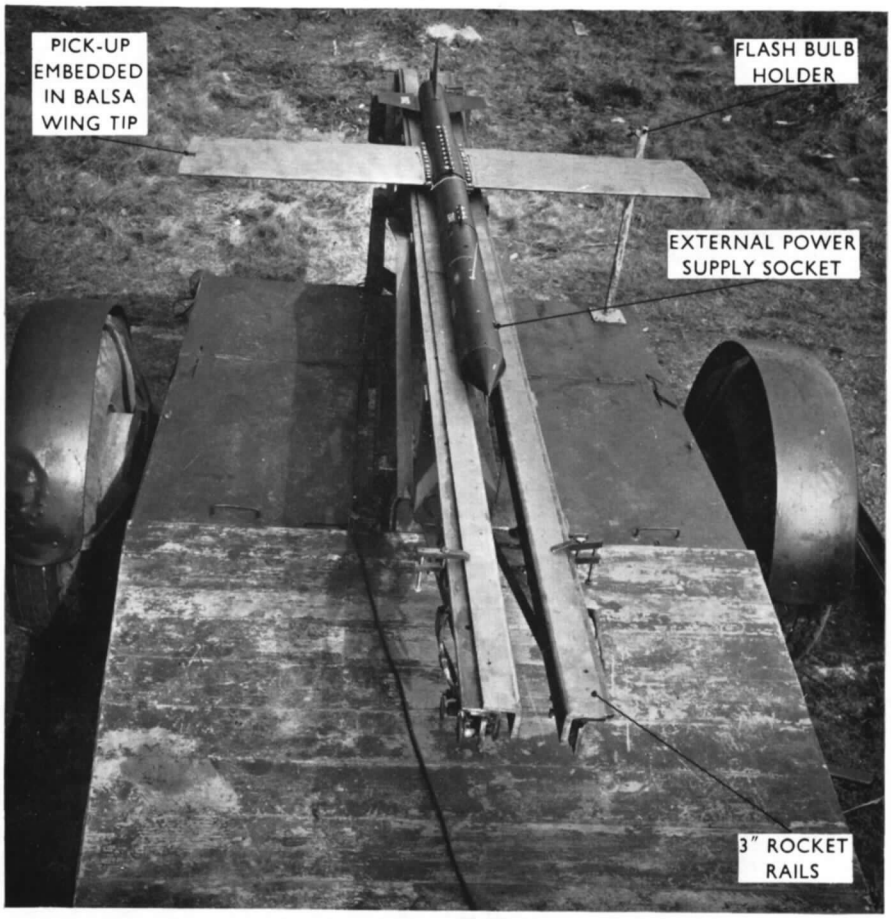

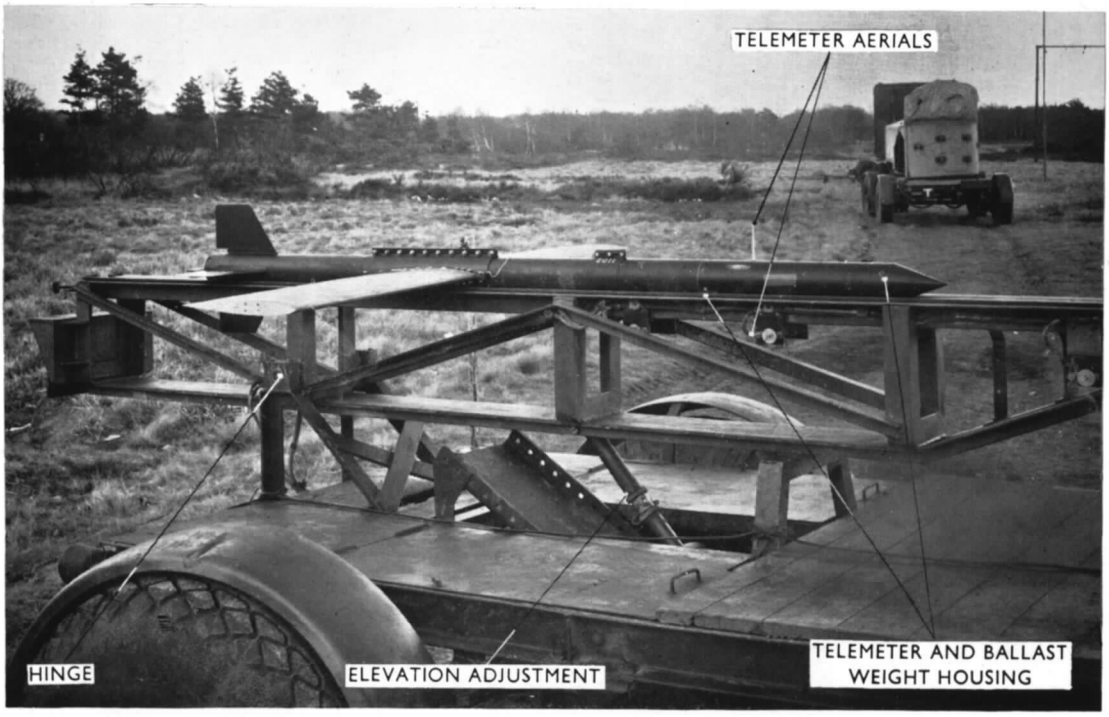

FIG. 2. Rocket model on launcher.

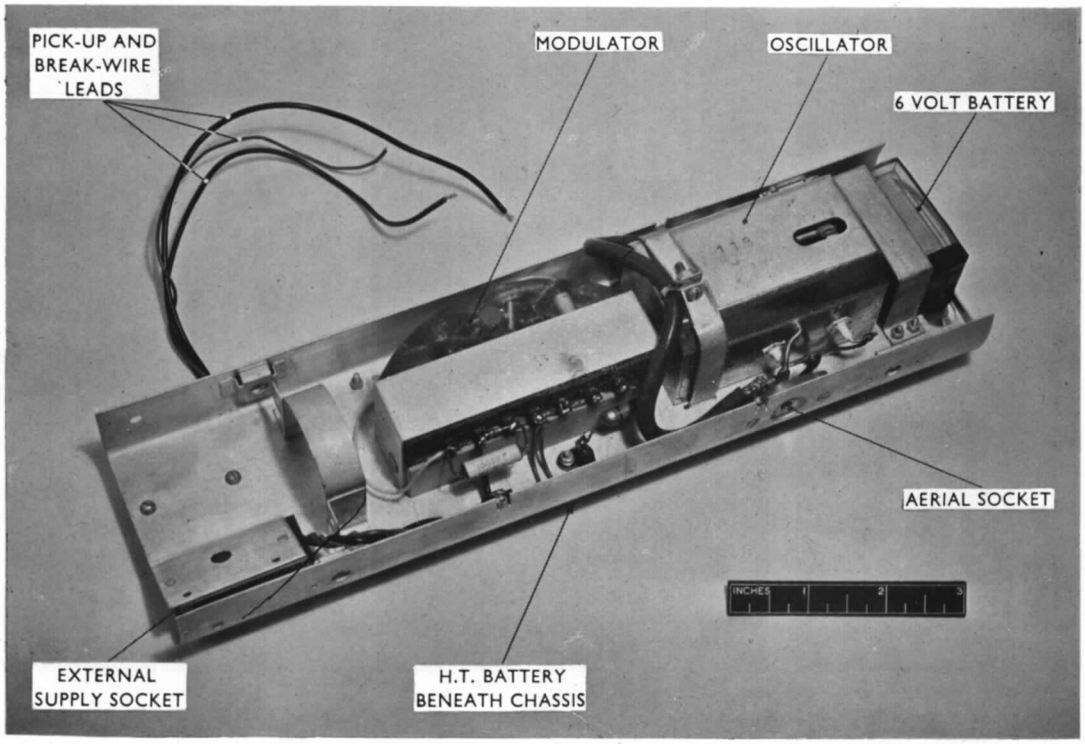

FIG. 3. Telemetry transmitter.

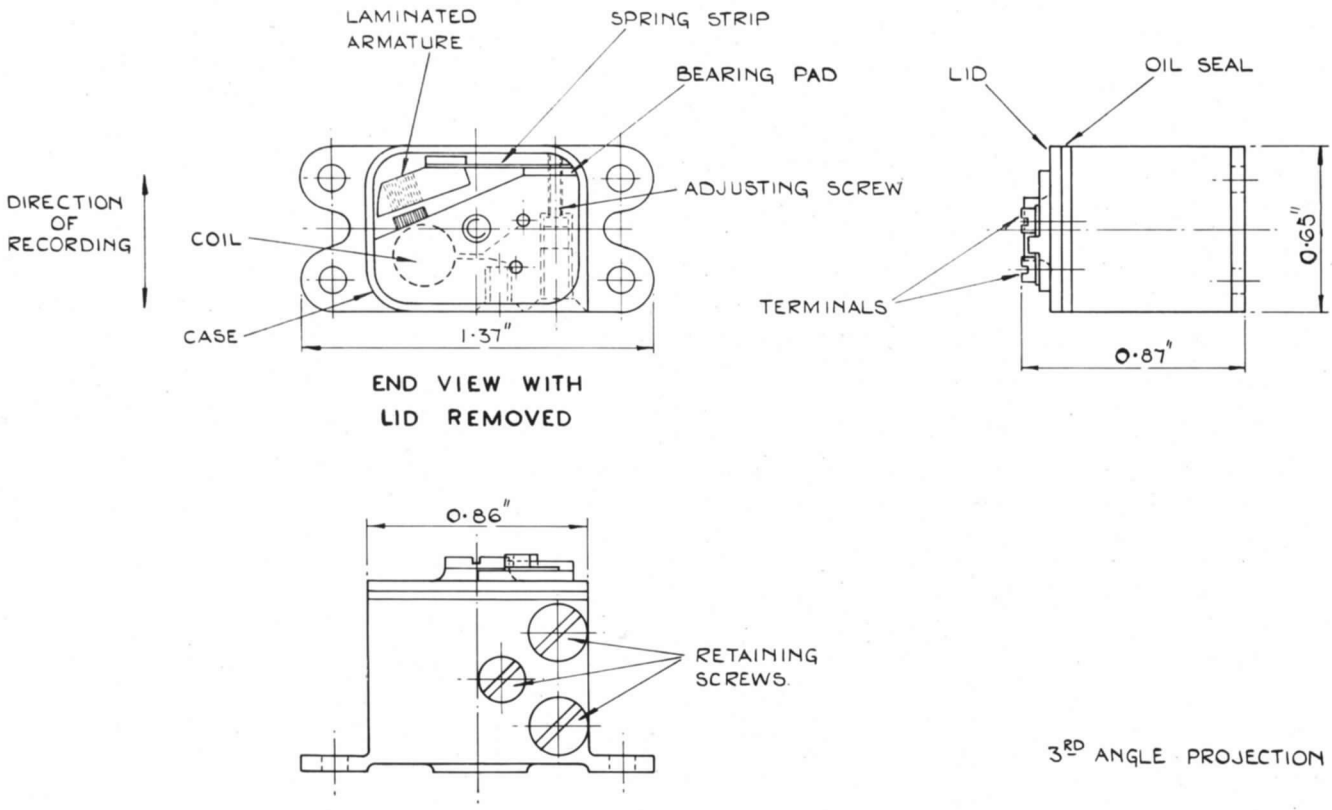

FIG. 4. General arrangement of vibration pick-up.

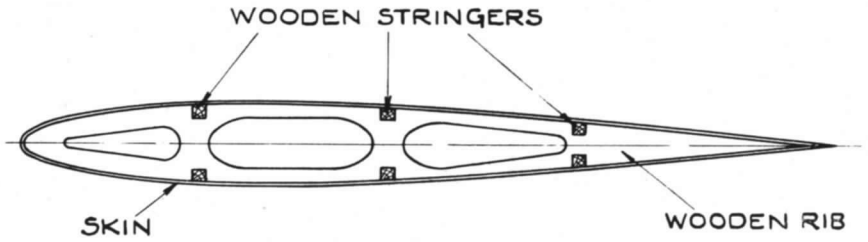

1. STRESSED SKIN CONSTRUCTION
(MODELS 1101 - 1115.)

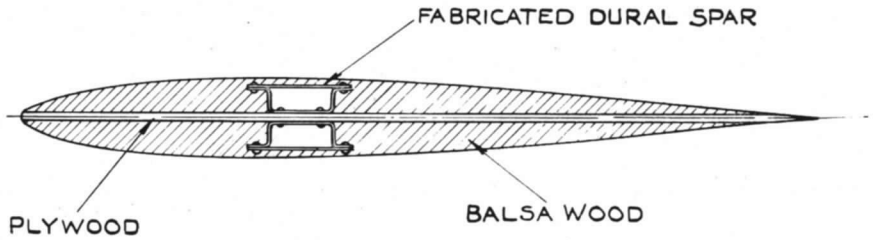

2. SOLID CONSTRUCTION.
(MODELS 1116-1128.)

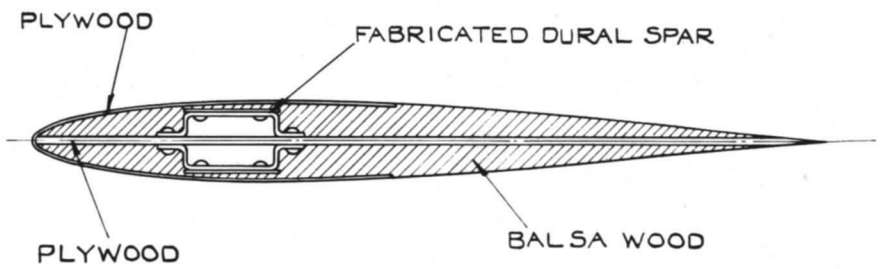

3. MODIFIED SOLID CONSTRUCTION.
(MODELS 1136-1143.)

FIG. 5. Wing construction details.

0·79 SECONDS AFTER LAUNCHING

0·80 SECONDS AFTER LAUNCHING

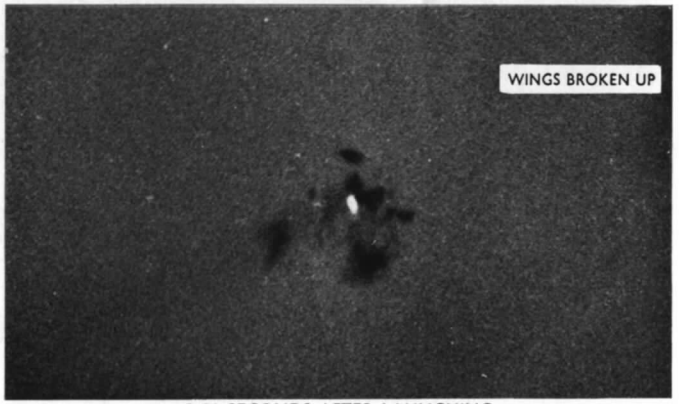

0·81 SECONDS AFTER LAUNCHING

FIG. 6. Camera record of flutter failure.

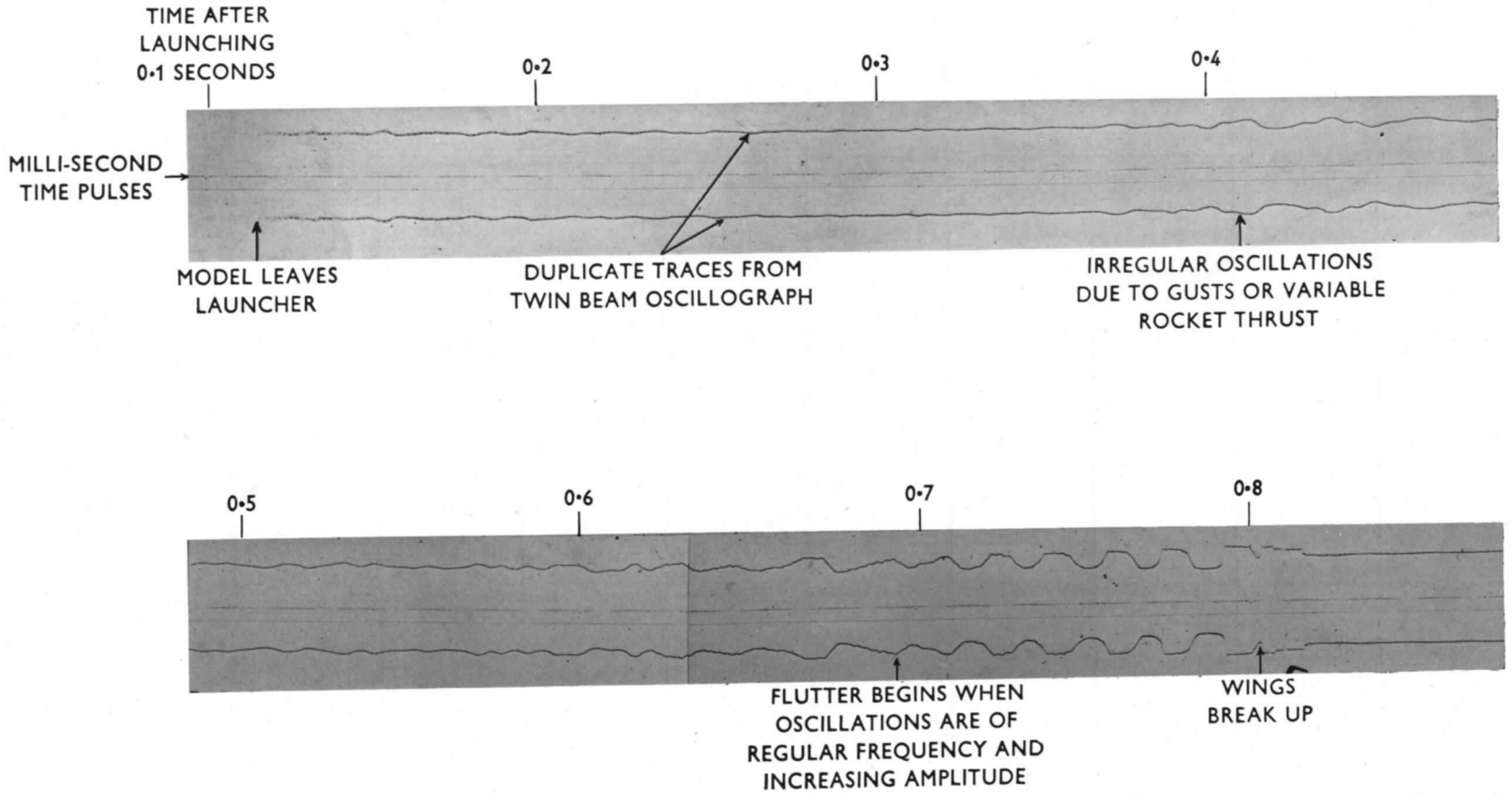

FIG. 7. Telemeter record of wing oscillations.

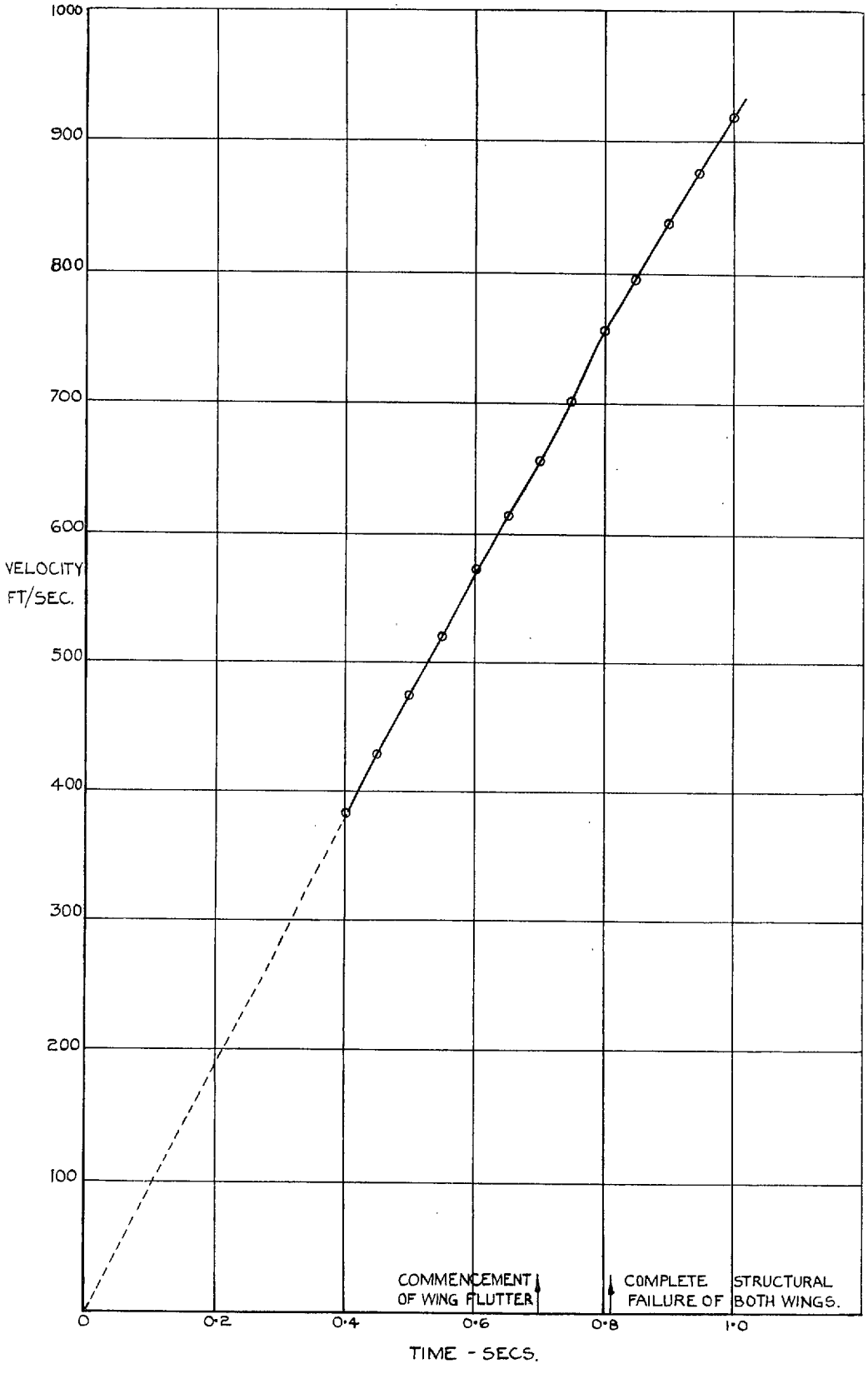

FIG. 8. Velocity-time curve from Doppler measurement.

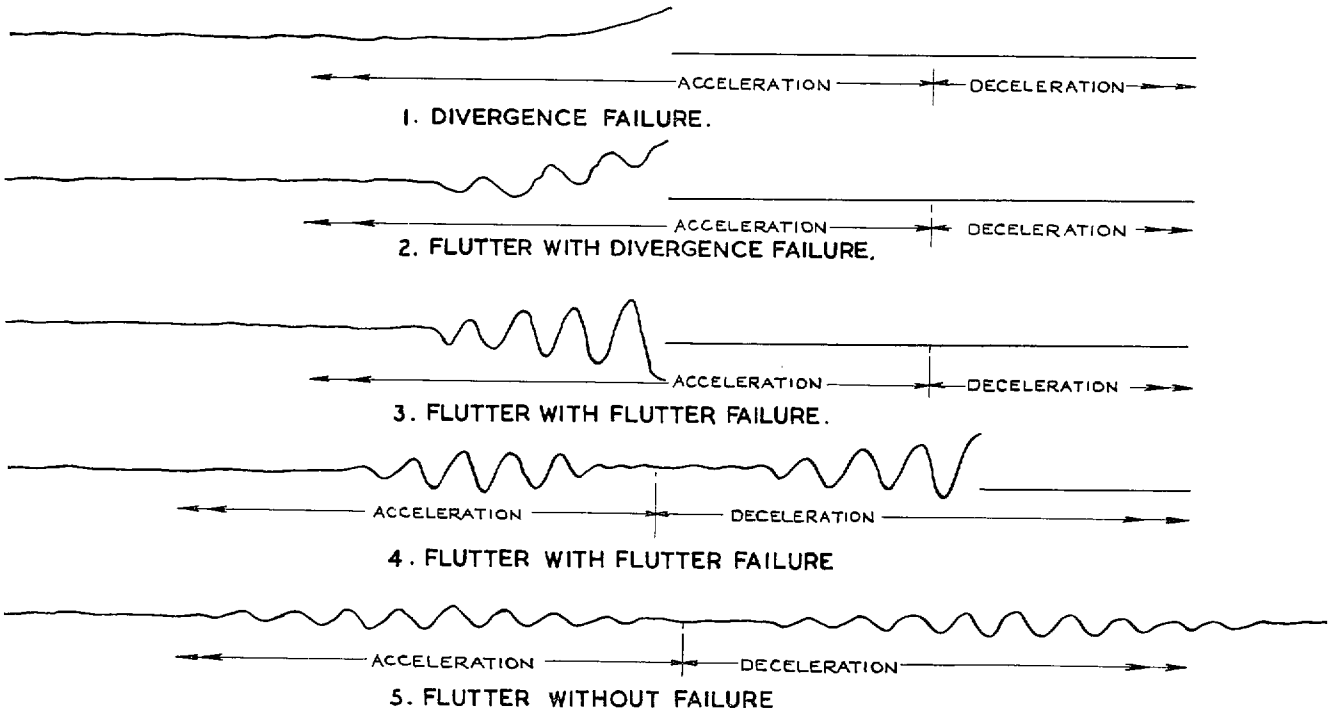

FIG. 9. Typical records of fiight characteristics.

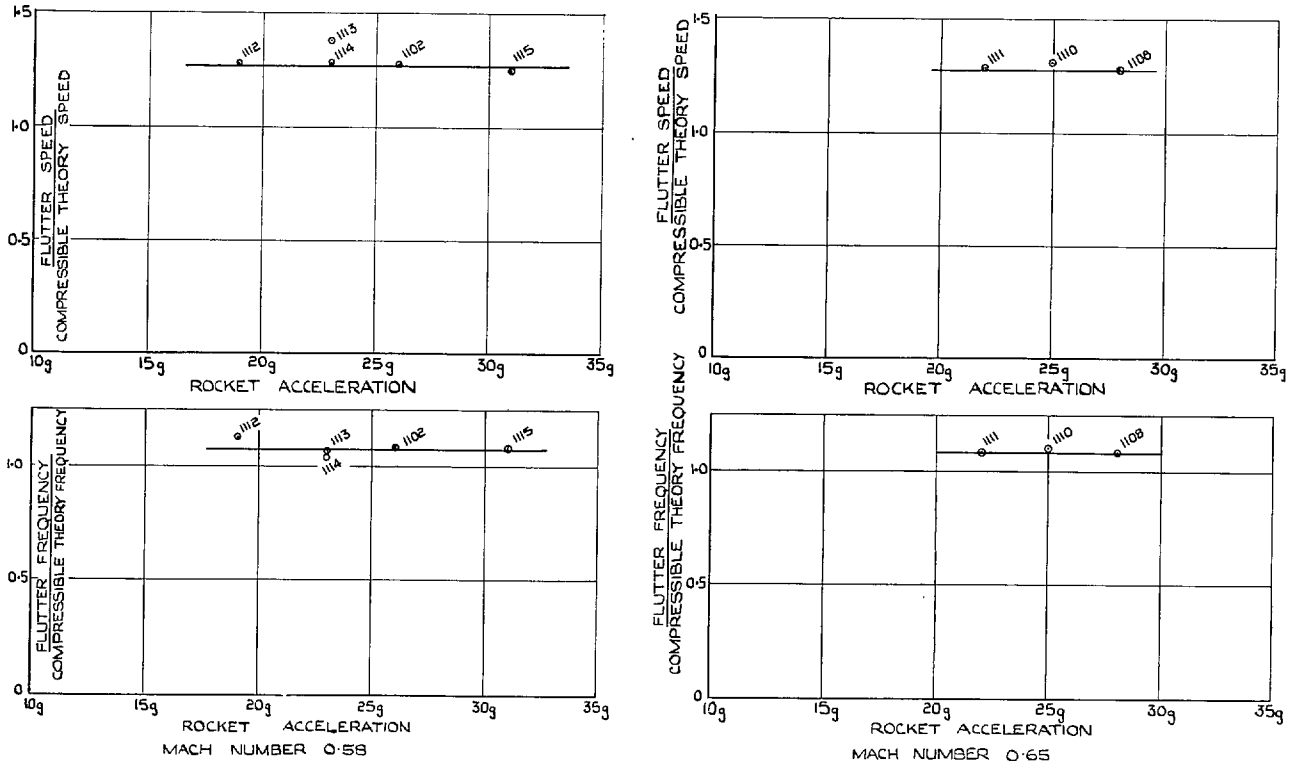

FIG. 10. Flutter speed and frequency ratios *vs.* acceleration at flutter.

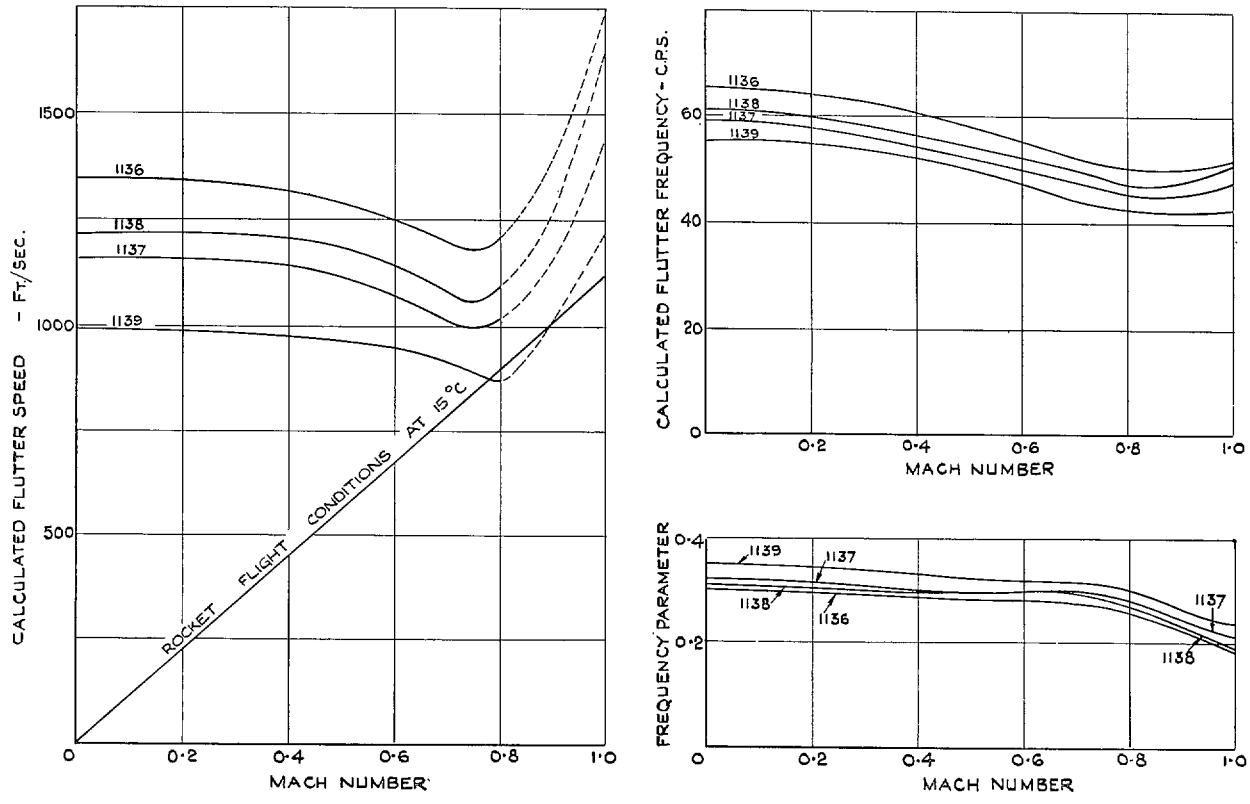

FIG. 11. Effect of compressibility on calculated flutter values (models 1136–1139)

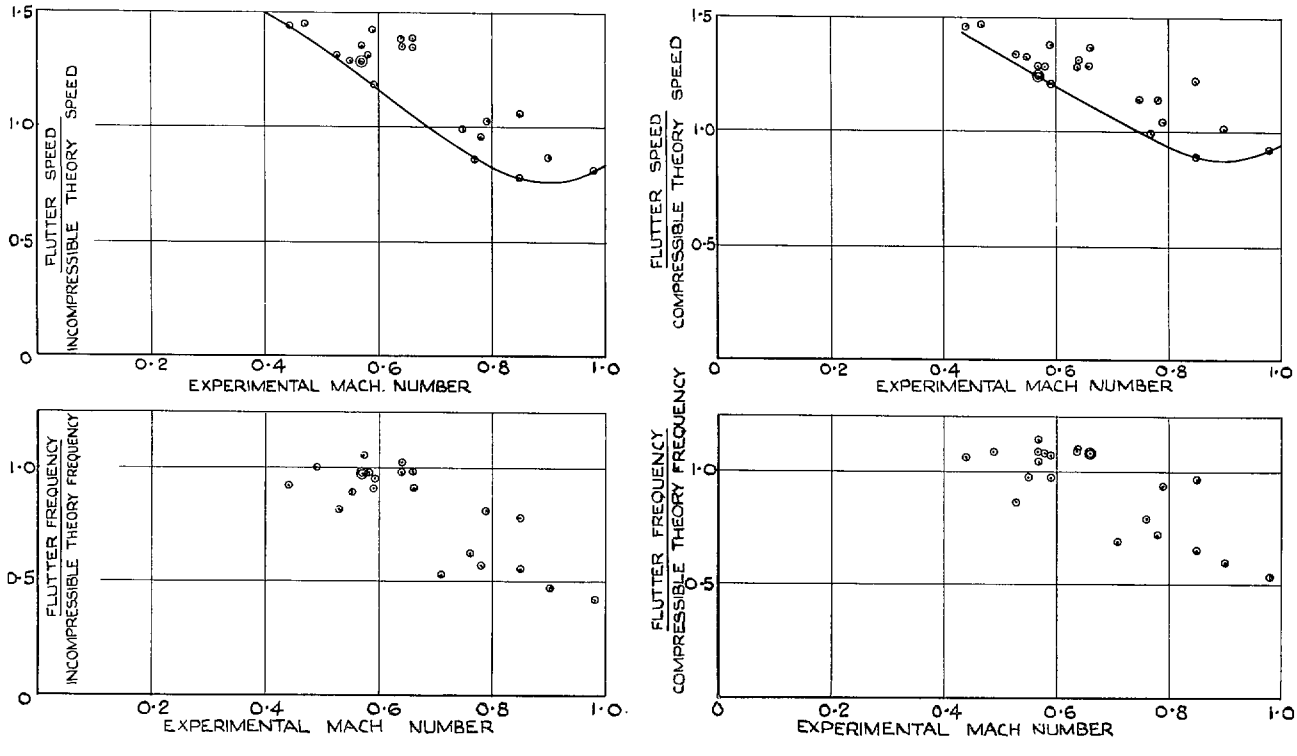

FIG. 12. Flutter speed and frequency ratios *vs.* Mach number at flutter

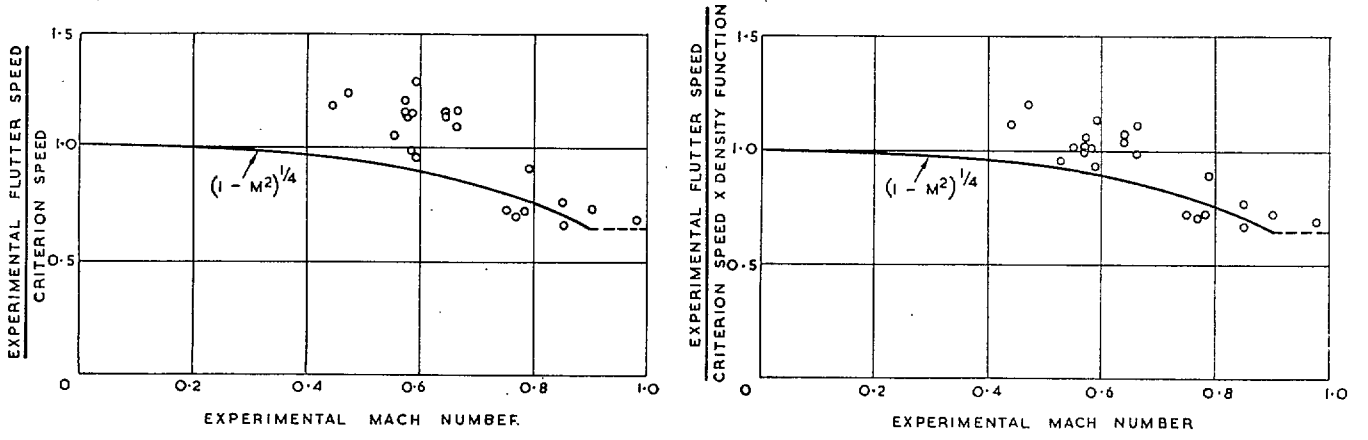

FIG. 13. Ratio of experimental flutter speed: criterion flutter speed *vs.* Mach number at flutter.

Wt. 18/9296 K.7 1/57 G.G. 34/262

PRINTED IN GREAT BRITAIN

Publications of the Aeronautical Research Council

ANNUAL TECHNICAL REPORTS OF THE AERONAUTICAL RESEARCH COUNCIL (BOUND VOLUMES)

1939 Vol. I. Aerodynamics General, Performance, Airscrews, Engines. 50*s.* (51*s.* 9*d.*)
Vol. II. Stability and Control, Flutter and Vibration, Instruments, Structures, Seaplanes, etc. 63*s.* (64*s.* 9*d.*)

1940 Aero and Hydrodynamics, Aerofoils, Airscrews, Engines, Flutter, Icing, Stability and Control, Structures, and a miscellaneous section. 50*s.* (51*s.* 9*d.*)

1941 Aero and Hydrodynamics, Aerofoils, Airscrews, Engines, Flutter, Stability and Control Structures. 63*s.* (64*s.* 9*d.*)

1942 Vol. I. Aero and Hydrodynamics, Aerofoils, Airscrews, Engines. 75*s.* (76*s.* 9*d.*)
Vol. II. Noise, Parachutes, Stability and Control, Structures, Vibration, Wind Tunnels. 47*s.* 6*d.* (49*s.* 3*d.*)

1943 Vol. I. Aerodynamics, Aerofoils, Airscrews. 80*s.* (81*s.* 9*d.*)
Vol. II. Engines, Flutter, Materials, Parachutes, Performance, Stability and Control, Structures. 90*s.* (92*s.* 6*d.*)

1944 Vol. I. Aero and Hydrodynamics, Aerofoils, Aircraft, Airscrews, Controls. 84*s.* (86*s* 3*d.*)
Vol. II. Flutter and Vibration, Materials, Miscellaneous, Navigation, Parachutes, Performance, Plates and Panels, Stability, Structures, Test Equipment, Wind Tunnels. 84*s.* (86*s.* 3*d.*)

1945 Vol. I. Aero and Hydrodynamics, Aerofoils. 130*s.* (132*s.* 6*d.*)
Vol. II. Aircraft, Airscrews, Controls. 130*s.* (132*s.* 6*d.*)
Vol. III. Flutter and Vibration, Instruments, Miscellaneous, Parachutes, Plates and Panels, Propulsion. 130*s.* (132*s.* 3*d.*)
Vol. IV. Stability, Structures, Wind Tunnels, Wind Tunnel Technique. 130*s.* (132*s.* 3*d.*)

Annual Reports of the Aeronautical Research Council—

1937 2*s.* (2*s.* 2*d.*) 1938 1*s.* 6*d.* (1*s.* 8*d.*) 1939–48 3*s.* (3*s.* 3*d.*)

Index to all Reports and Memoranda published in the Annual Technical Reports, and separately—

April, 1950 R. & M. 2600. 2*s.* 6*d.* (2*s.* 8*d.*)

Author Index to all Reports and Memoranda of the Aeronautical Research Council—

1909–January, 1954. R. & M. No. 2570 15*s.* (15*s.* 6*d.*)

Indexes to the Technical Reports of the Aeronautical Research Council—

December 1, 1936 — June 30, 1939.	R. & M. No. 1850.	1*s.* 3*d.* (1*s.* 5*d.*)
July 1, 1939 — June 30, 1945.	R. & M. No. 1950.	1*s.* (1*s.* 2*d.*)
July 1, 1945 — June 30, 1946	R. & M. No. 2050.	1*s.* (1*s.* 2*d.*)
July 1, 1946 — December 31, 1946.	R. & M. No. 2150.	1*s.* 3*d.* (1*s.* 5*d.*)
January 1, 1947 — June 30, 1947.	R. & M. No. 2250.	1*s.* 3*d.* (1*s.* 5*d.*)

Published Reports and Memoranda of the Aeronautical Research Council—

Between Nos. 2251–2349	R. & M. No. 2350.	1*s.* 9*d.* (1*s.* 11*d.*)
Between Nos. 2351–2449	R. & M. No. 2450.	2*s.* (2*s.* 2*d.*)
Between Nos. 2451–2549	R. & M. No. 2550.	2*s.* 6*d.* (2*s.* 8*d.*)
Between Nos. 2551–2649	R. & M. No. 2650.	2*s.* 6*d.* (2*s.* 8*d.*)

Prices in brackets include postage

HER MAJESTY'S STATIONERY OFFICE

York House, Kingsway, London W.C.2; 423 Oxford Street, London W.1 (Post Orders: P.O. Box 569, London S.E.1); 13a Castle Street, Edinburgh 2; 39 King Street, Manchester 2; 2 Edmund Street, Birmingham 3; 109 St. Mary Street, Cardiff; Tower Lane, Bristol 1; 80 Chichester Street, Belfast, or through any bookseller

S.O. Code No. 23-2944